

Anionic Effect on Electrical Transport Properties of Solid Co^{2+/3+} Redox Mediators

Ravindra Kumar Gupta *, Ahamad Imran and Aslam Khan

King Abdullah Institute for Nanotechnology, King Saud University, Riyadh 11451, Saudi Arabia

* Correspondence: rgupta@ksu.edu.sa

Supplementary Information

Table S1. Abbreviations used in the article.

ACN, acetonitrile
SN, succinonitrile
PEO, poly(ethylene oxide)
bpy, tris-(2,2'-bipyridine)
TFSI, bis(trifluoromethyl) sulfonylimide
Triflate, trifluoromethanesulfonate
DSSC, dye-sensitized solar cell
SRM, solid redox mediator
LRM, liquid redox mediator
IS, impedance spectroscopy
FT-IR, Fourier-transform infrared spectroscopy
XRD, X-ray diffractometry
XPS, X-ray photoelectron spectroscopy
SEM, scanning electron microscopy
UV-vis, UV-visible spectroscopy
DSC, differential scanning calorimetry
TGA, thermogravimetric analysis
σ , electrical conductivity
R_b , bulk resistance
R_s , series resistance due to leads
C_1 , chemical capacitance
C_2 , double-layer capacitance
E_a , activation energy
σ_0 , pre-exponential factor
k_B , Boltzmann constant
B , pseudo-activation energy
T_0 , free-volume temperature
T_m , melting temperature
T_{pc} , crystal-to-plastic-crystal phase transition temperature
I_{1105} , intensity at 1105 cm ⁻¹ for the $\nu_{s,COC}$ mode of PEO
I_{1196} , intensity at 1196 cm ⁻¹ for the $\nu_{a,CF3}$ mode of ionic salts
$\Delta I = I_{1105}/I_{1196}$
R = intensity/width
$\Delta R = R_{TFSI} - R_{Triflate}$
ΔP = Peak Position _{TFSI} – Peak Position _{Triflate}

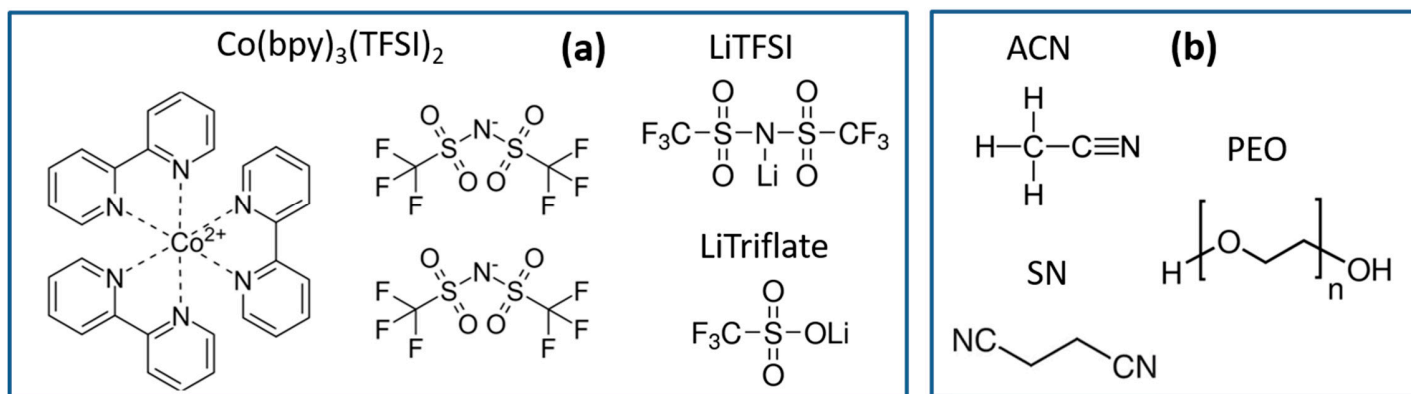


Figure S1. Chemical structure of (a) ionic salts and (b) matrices.

Table S2. Chemicals used for the preparation of liquid and solid redox mediators.

Chemicals	Purity (%)	Make
Acetonitrile (ACN)	99.9	Fisher Scientific, USA
Succinonitrile	99	Sigma-Aldrich, Inc., USA
Poly(ethylene oxide)	99	Sigma-Aldrich, Inc., USA
Li(CF ₃ SO ₂) ₂ N	99.9	Sigma-Aldrich, Inc., USA
LiCF ₃ SO ₃	96	Sigma-Aldrich, Inc., USA
Co(bpy) ₃ (TFSI) ₂	-	Dyenamo, Sweden
Co(bpy) ₃ (TFSI) ₃	-	Dyenamo, Sweden

Table S3. Details of characterization techniques.

Technique	Details
IS	We poured a liquid electrolyte (LRM or SRM with $x = 0$ in liquid form) into the space of a sample holder [1]. This space with an area (A) of 0.16 cm ² and a thickness (l) of 0.05 cm was produced by a Teflon spacer between platinum plates (the blocking electrode). We placed a thick film of PEO-based SRMs ($x = 0.5$ and 1) between the stainless steel plates (blocking electrode; diameter = 1 cm) of another sample holder [2]. The electrolyte was subjected to a 20 mV AC voltage with a frequency range of 10 ⁵ -1 Hz using an impedance analyzer. The resulting Nyquist curve helped to deduce the bulk resistance and, thereby, the electrical conductivity. The temperature-dependent measurement of electrical conductivity helped to determine the activation energy.
FT-IR	We formed a thin film of electrolyte on a KBr pellet (diameter 2.5 cm; thickness 0.2 cm). We collected the FT-IR spectrum of this film from 4000 to 400 cm ⁻¹ with a resolution of 1 cm ⁻¹ at 25 °C using an FT-IR spectrometer.
XRD	A thick film of electrolyte was formed on a cover glass (area 1 cm ²). This film was subjected to CuK α radiation (1.54184 Å) in a range of 10–40° with a step of 0.06° using a diffractometer. The amorphous profile was smoothed to decrease the noise-to-signal ratio.
XPS	A mesoporous TiO ₂ (size 18 nm) layer with an area of 1 cm ² and thickness of 7 µm on a microscopic glass was coated with the electrolyte. We subjected this film to MgK α X-ray radiation (1253.6 eV) under ultra-high vacuum conditions using an XPS unit. We scanned the film five times, from 1000 to 0 eV, using a step of 1 eV to survey the elements. We precisely determined the elements' position by scanning ten times at a step of 0.1 eV for 100 ms. The spectra of elements were corrected to fix the C 1s peak at 284.6 eV, smoothed for 5 points, and finally corrected for the rubberband baseline. We used software to perform the best fit and deconvolute the peak. The intensity of the peak was divided by the width (full width at half maxima) to make the ratio dimensionless.
SEM	A film of electrolyte was formed on a mesoporous TiO ₂ layer (thickness 7 µm) on a microscopic glass (area 1 cm ²). This glass was broken into small pieces. A very small piece of this film was coated with platinum using a JEOL DC sputtering unit, and an image was obtained using a JEOL scanning electron microscope.
UV-vis	We formed a micron-thick electrolyte film on a cover glass (area 1.5 cm ²). We recorded the transmittance spectrum of the film using a UV-visible spectrometer.
DSC	We sealed an aluminum crucible containing nearly 10 mg of electrolyte. This crucible was subjected to heat flow measurement from –50 °C to 90 °C at 10 °C per minute using a DSC unit in the N ₂ gas environment.
TGA	We covered an alumina pan containing nearly 10 mg of electrolyte and used a TGA unit in a nitrogen gas environment to measure the weight loss from room temperature to 600 °C at 10 °C per minute.

Table S4. Equipment used for the measurements.

Technique	Equipment
IS	Model PalmSens4, Palmsens impedance analyzer, Houten, the Netherlands
FT-IR	Model Spectrum 100, Perkin Elmer FT-IR spectrometer, Waltham, USA
XRD	Model D2 Phaser, Bruker X-ray diffractometer, Karlsruhe, Germany
XPS	Model JPS-9030, JEOL X-ray photoelectron spectrometer, Tokyo, Japan
SEM	Model JSM-7600F, JEOL scanning electron microscope, Tokyo, Japan
UV-vis	Model 8453, Agilent UV-visible spectrometer, Santa Clara, USA
DSC	Model DSC-60A, Shimadzu differential scanning calorimeter, Kyoto, Japan
TGA	Model DTG-60H, Shimadzu TGA unit, Kyoto, Japan

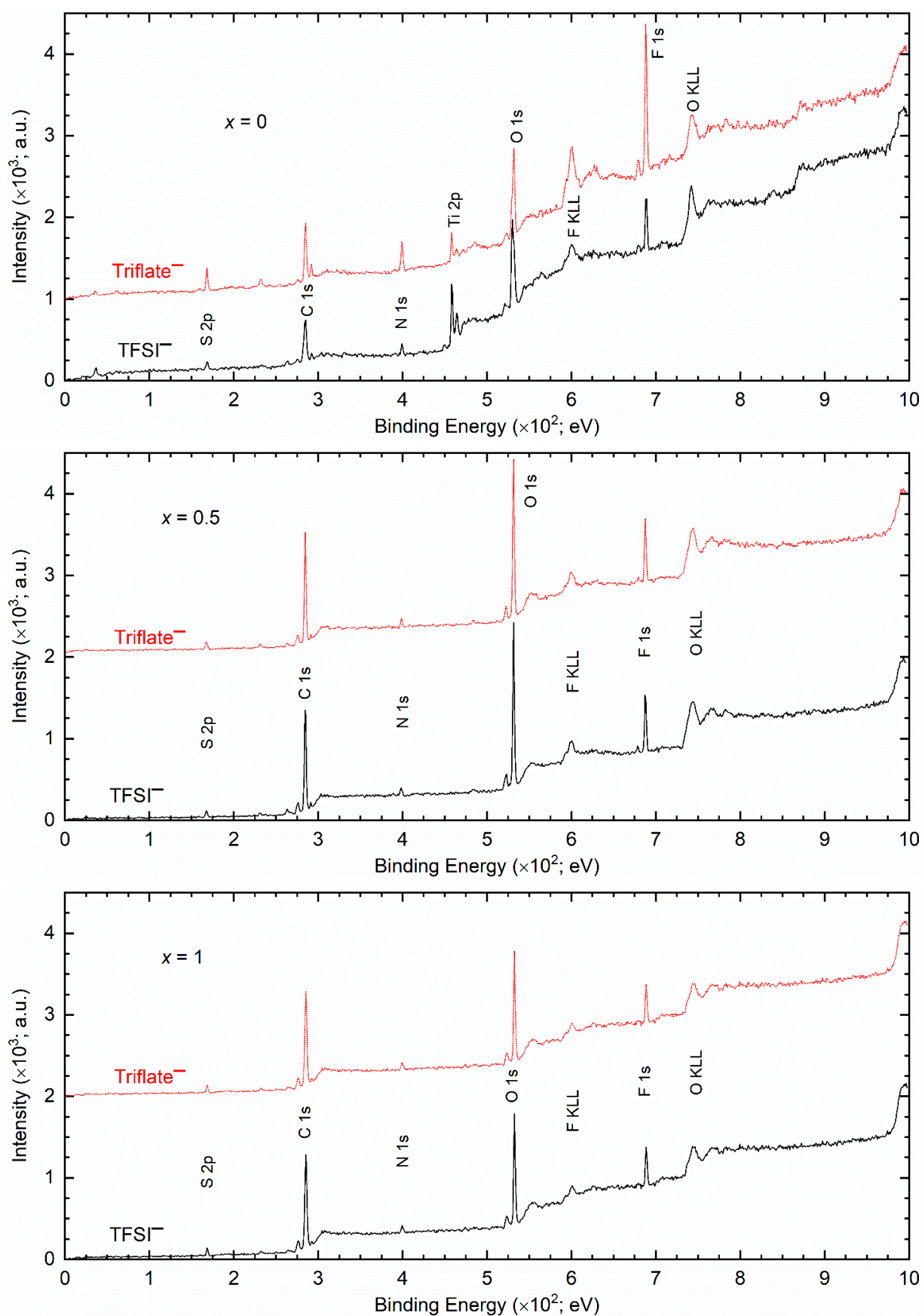
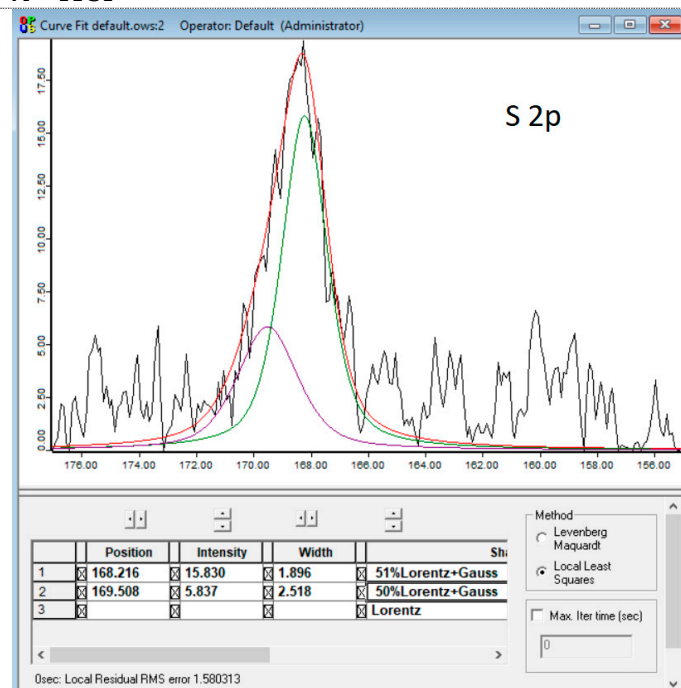


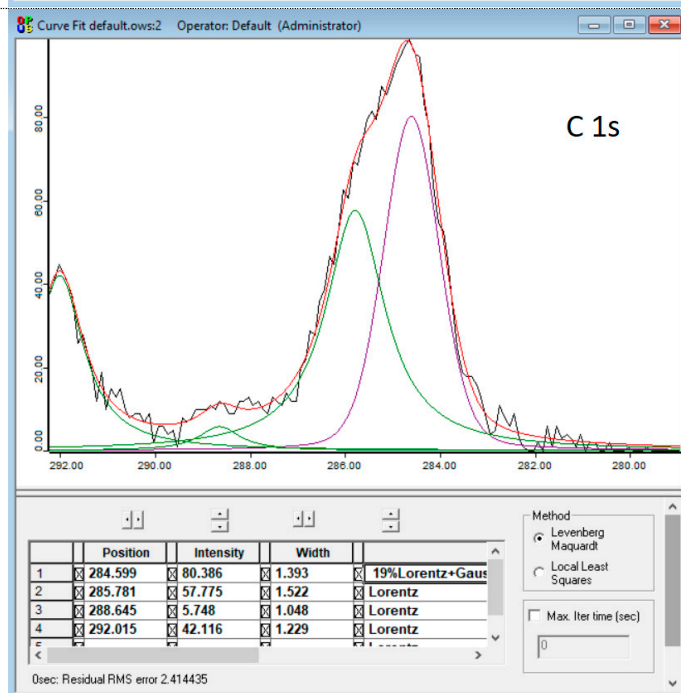
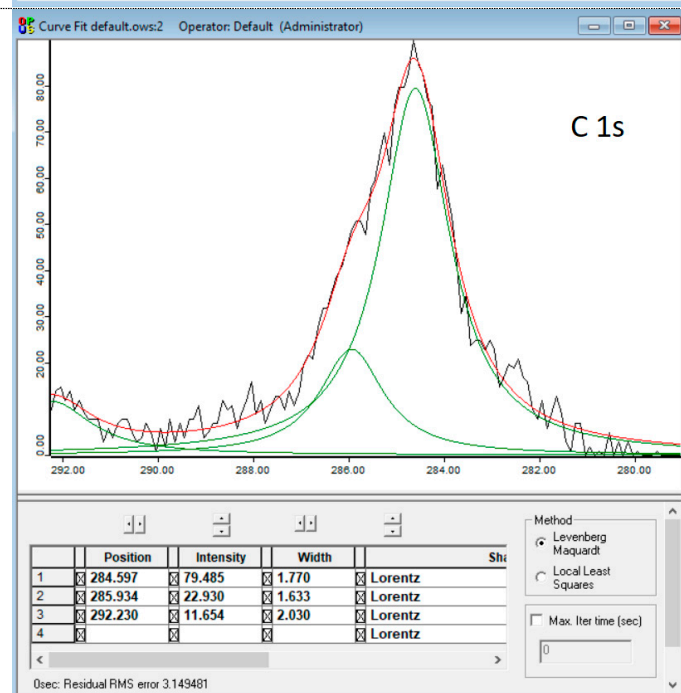
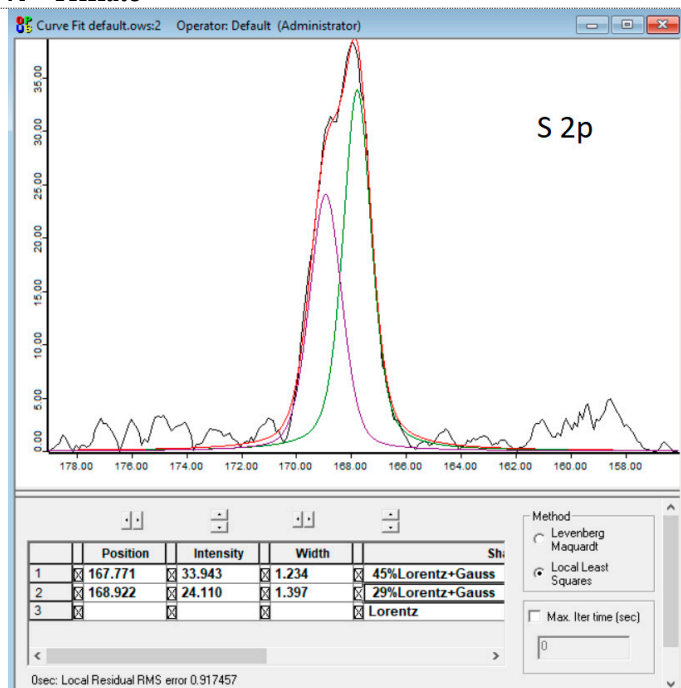
Figure S2. XPS survey spectra of solid redox mediators, $[(1-x)\text{SN}: x\text{PEO}]\text{-LiX-Co}$ salts ($x = 0, 0.5$, and 1 ; $X = \text{TFSI}^-$ and Triflate^-).

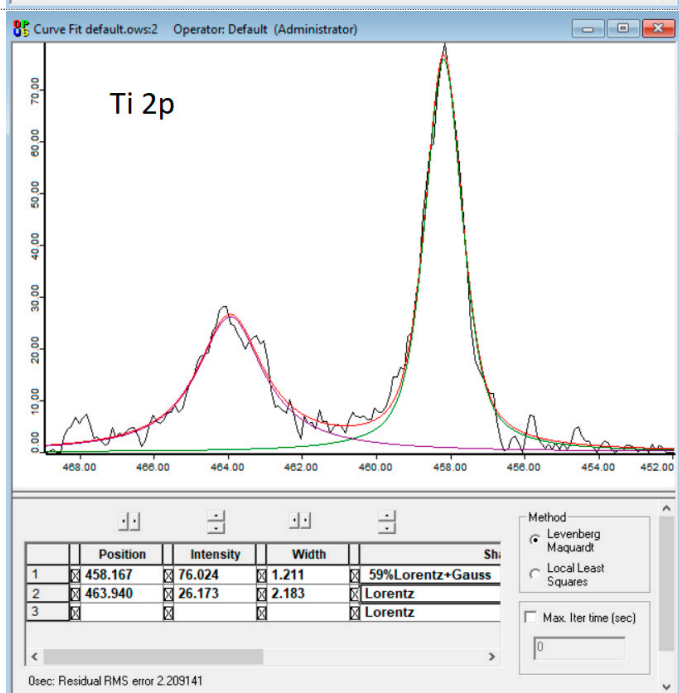
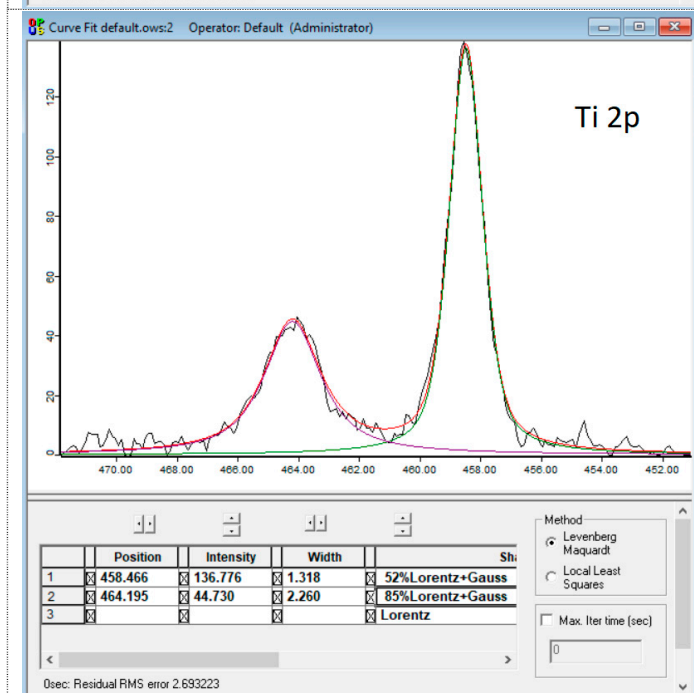
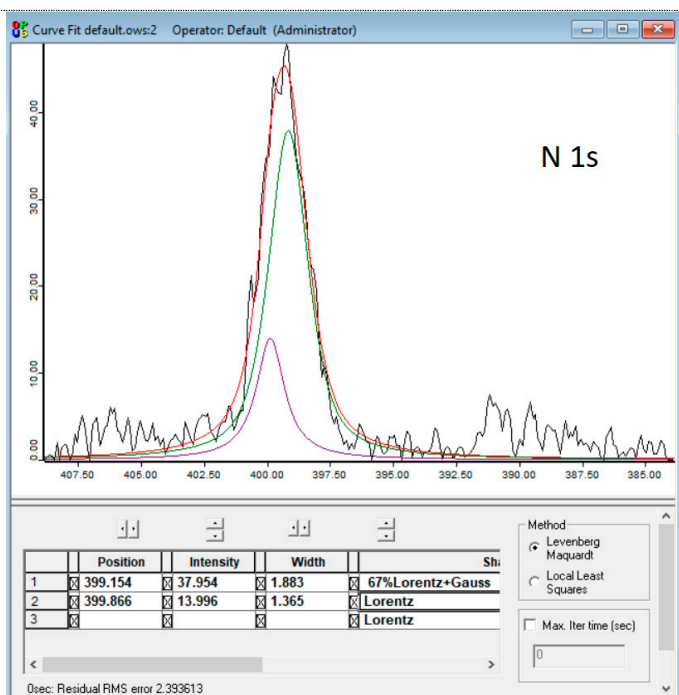
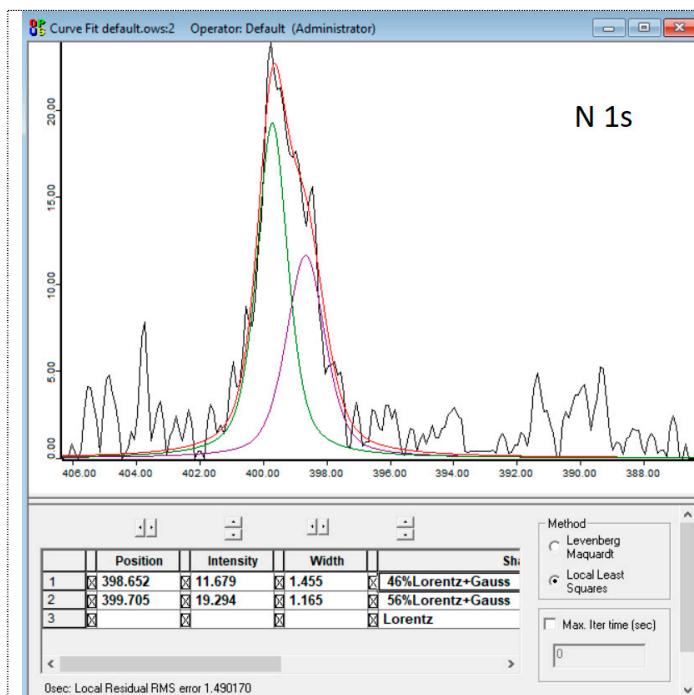
$x = 0$

X = TFSI⁻



X = Triflate⁻





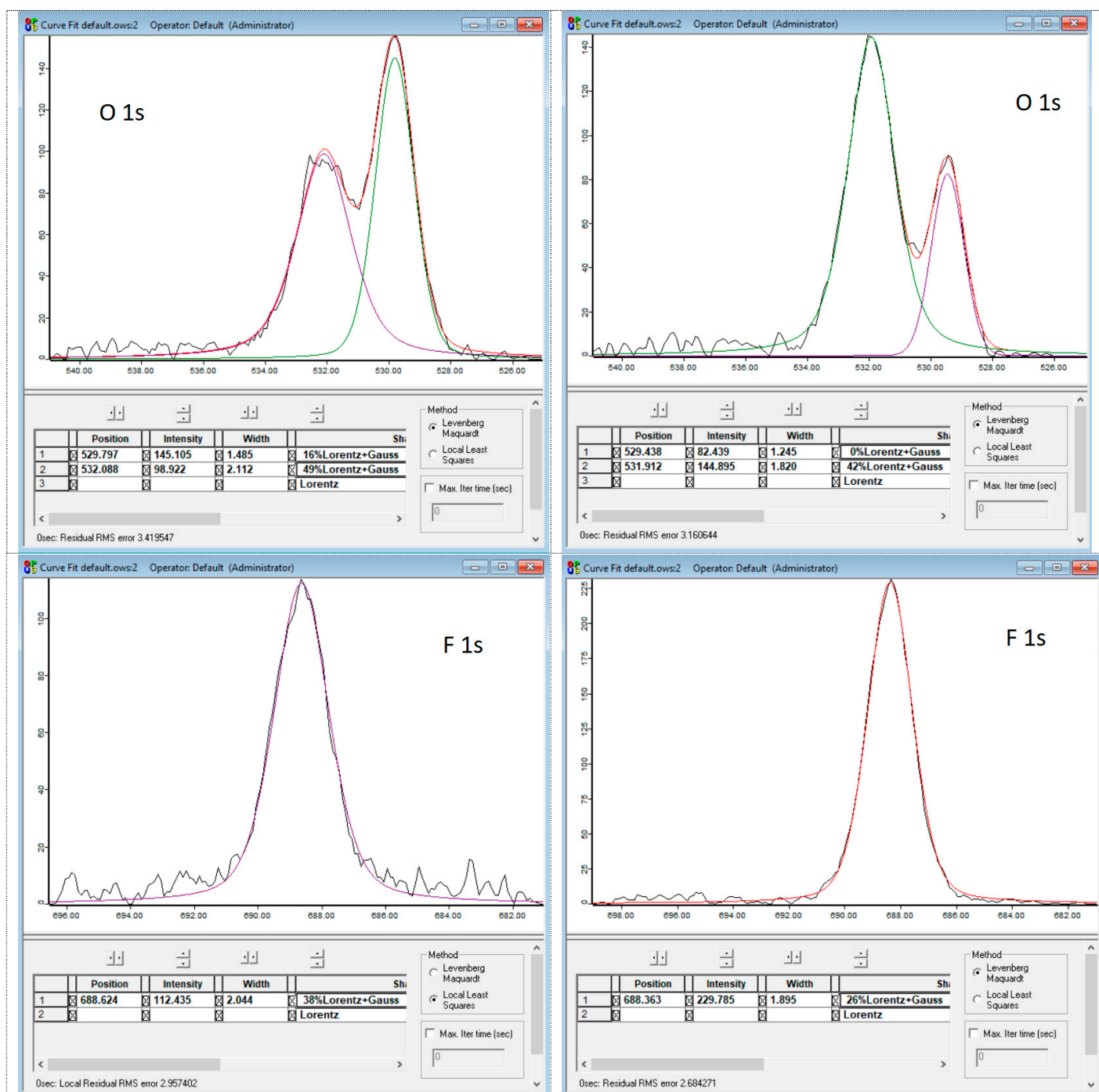
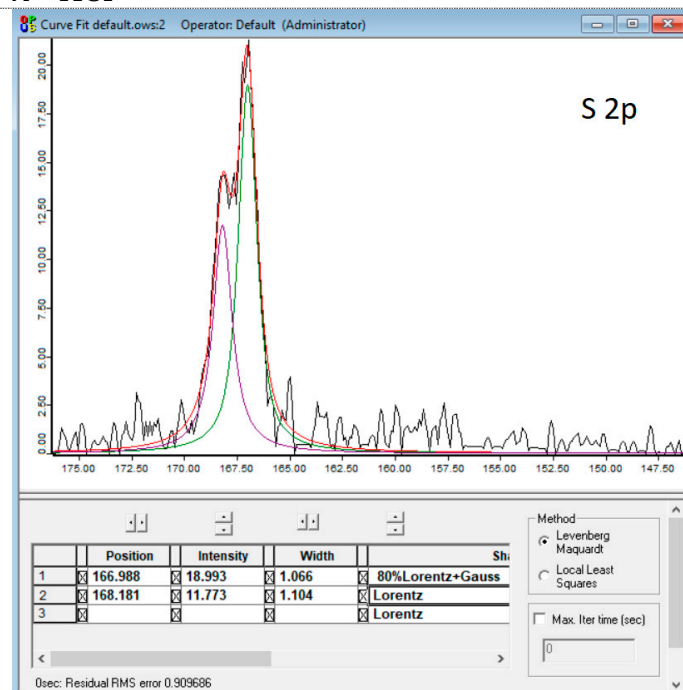


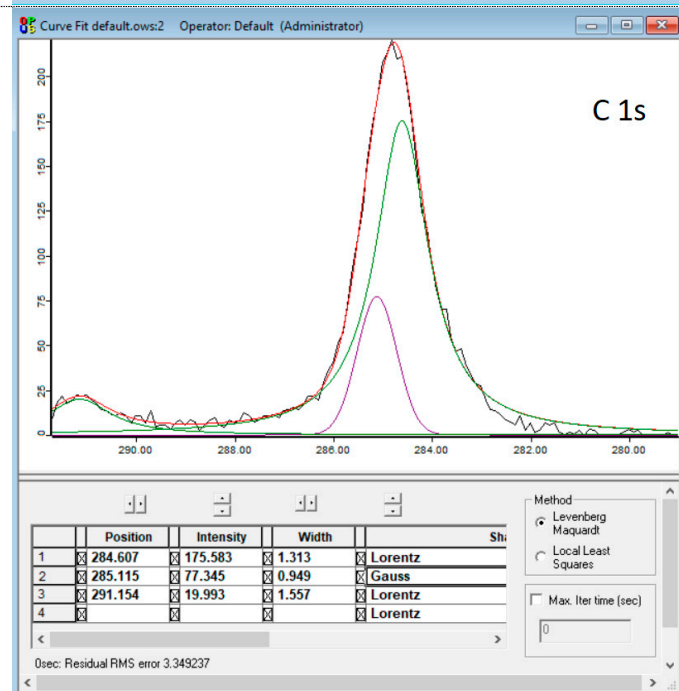
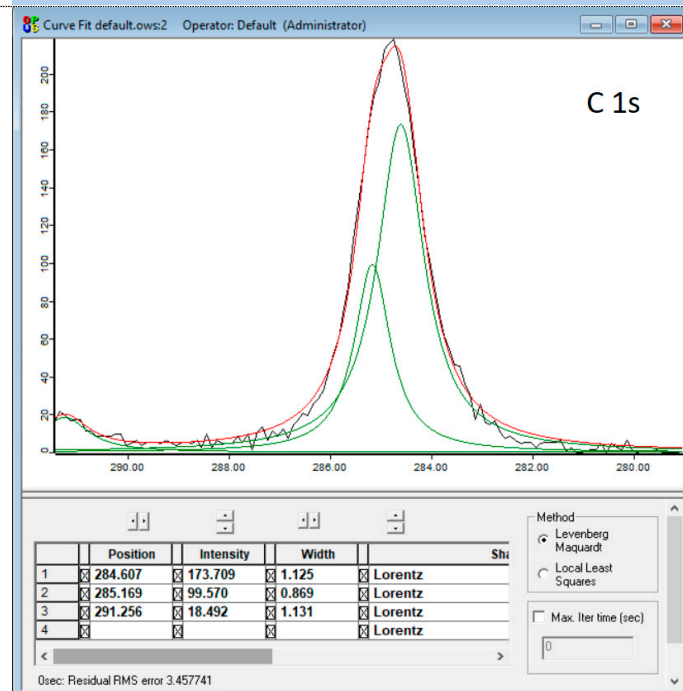
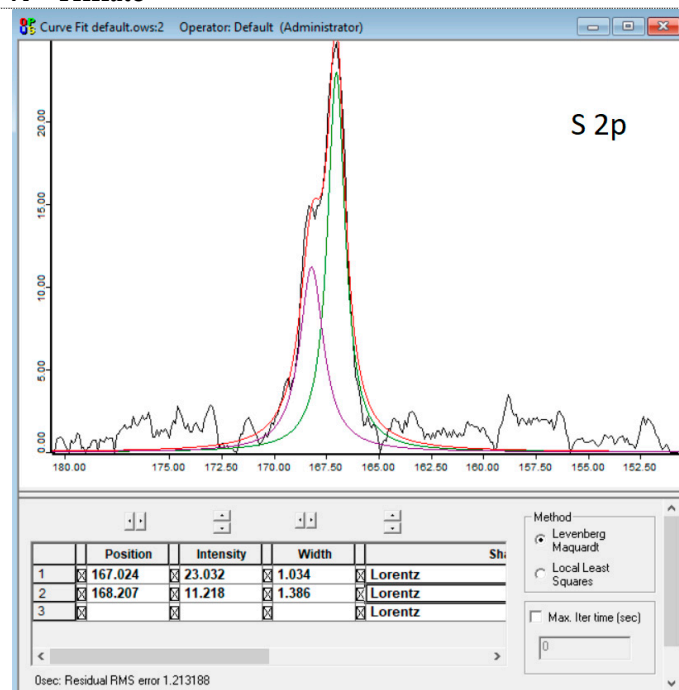
Figure S3. Best fits of XPS spectra of different elements of solid redox mediators ($x = 0$; $X = \text{TFSI}^-$ and Triflate^-). This figure also includes the best fits of XPS spectra of the Ti 2p element.

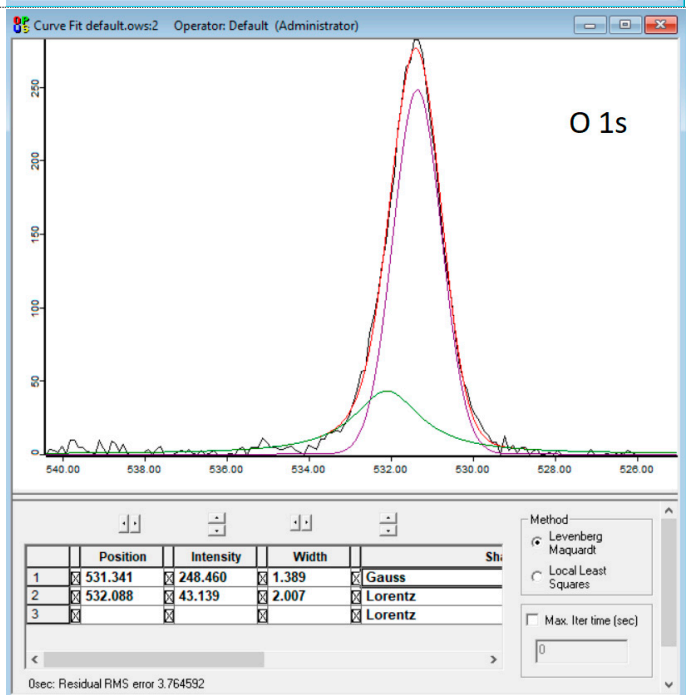
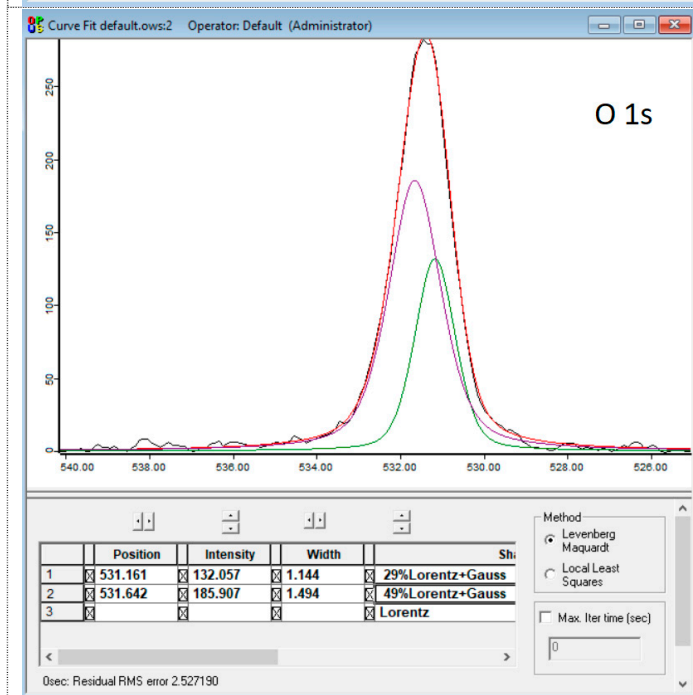
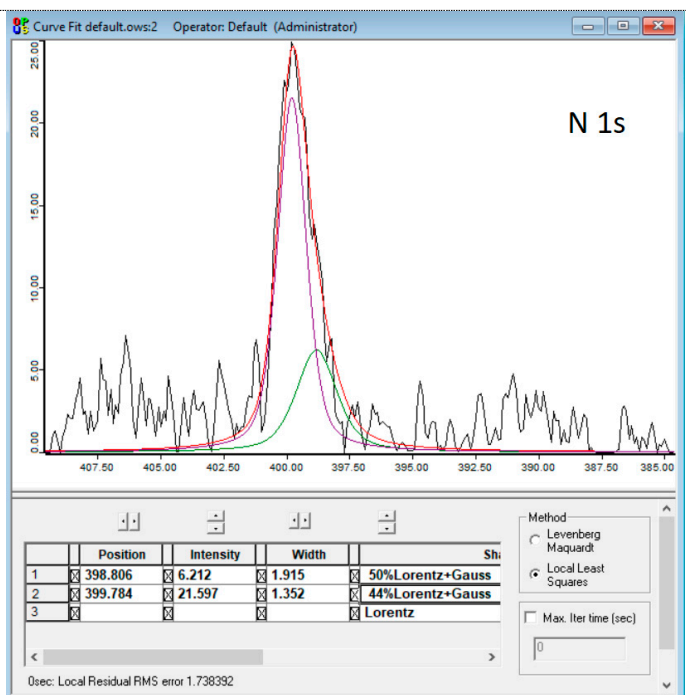
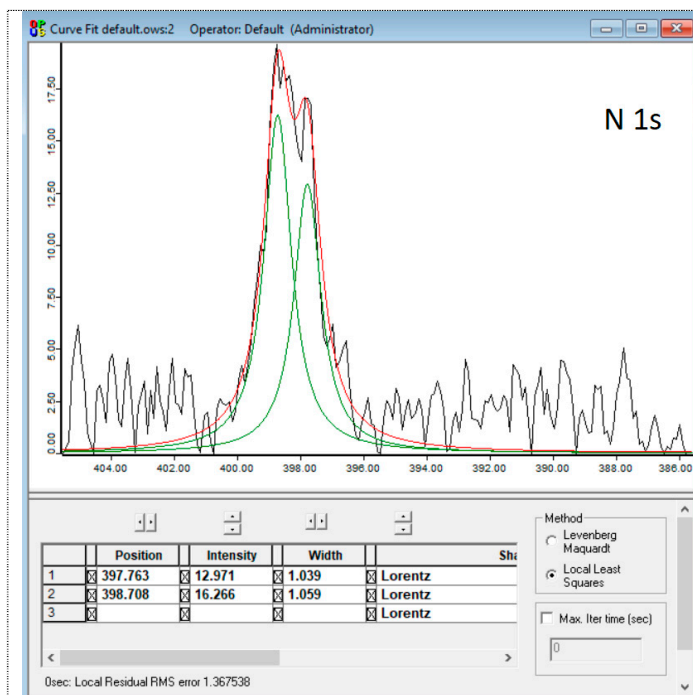
$\alpha = 0.5$

X = TFSI⁻



X = Triflate⁻





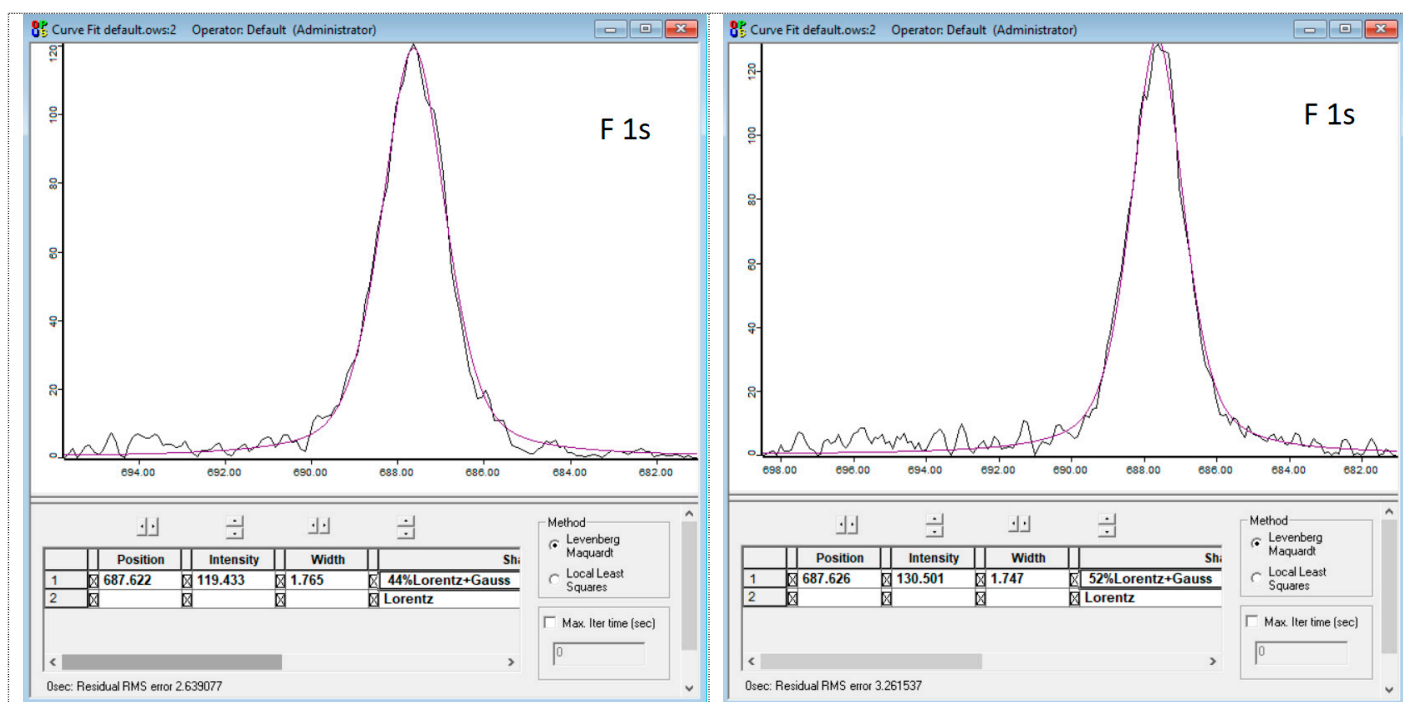
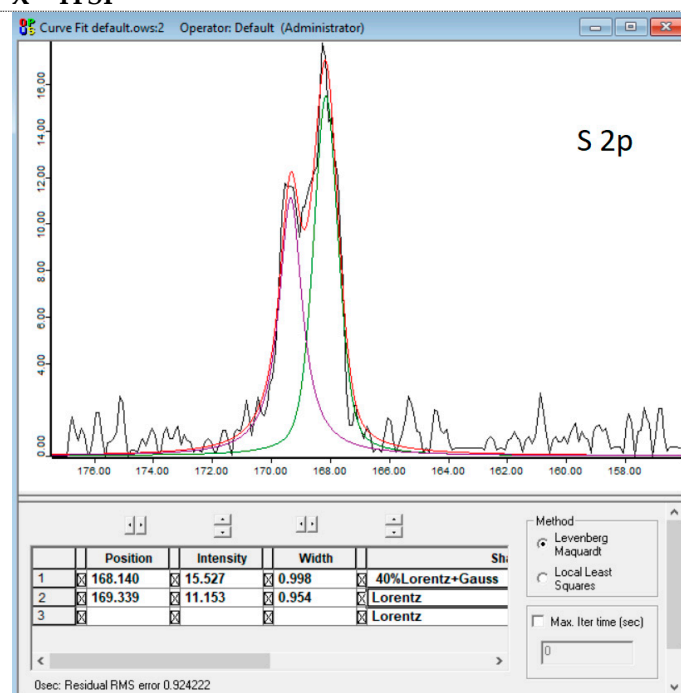


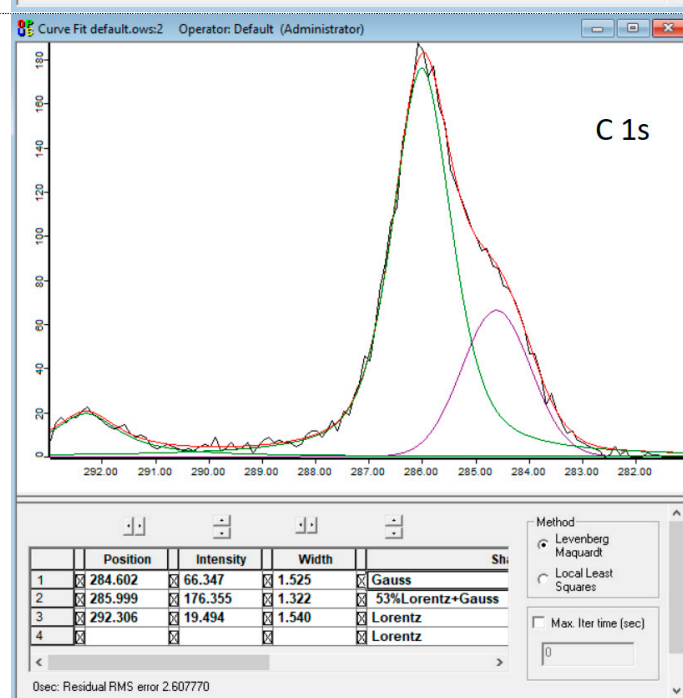
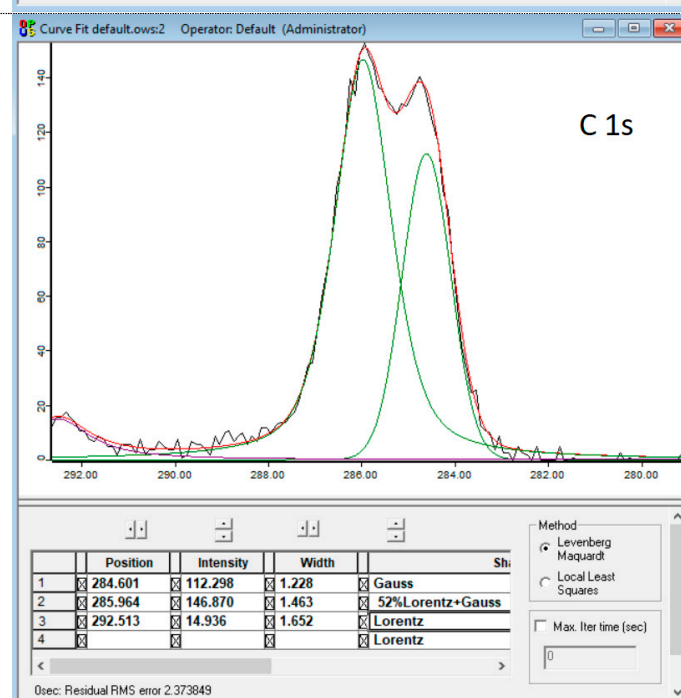
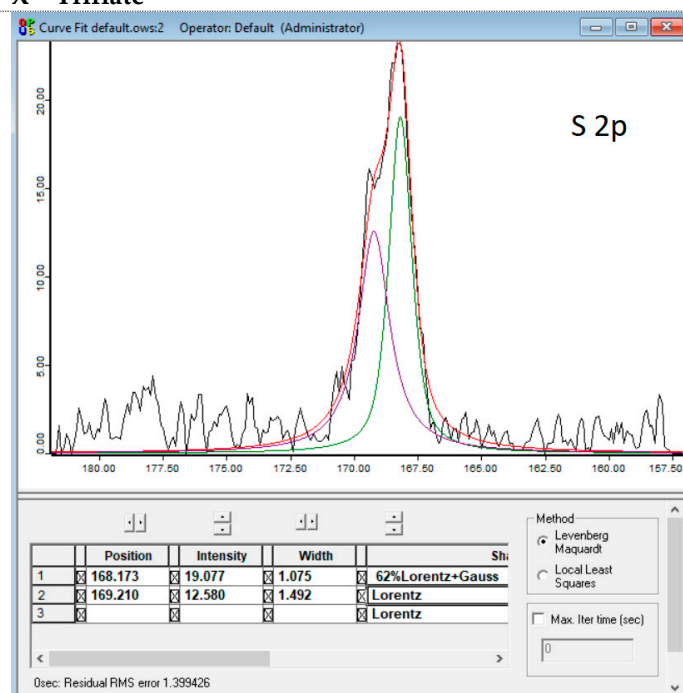
Figure S4. Best fits of XPS spectra of different elements of solid redox mediators ($\chi = 0.5$; X = TFSI⁻ and Triflate⁻).

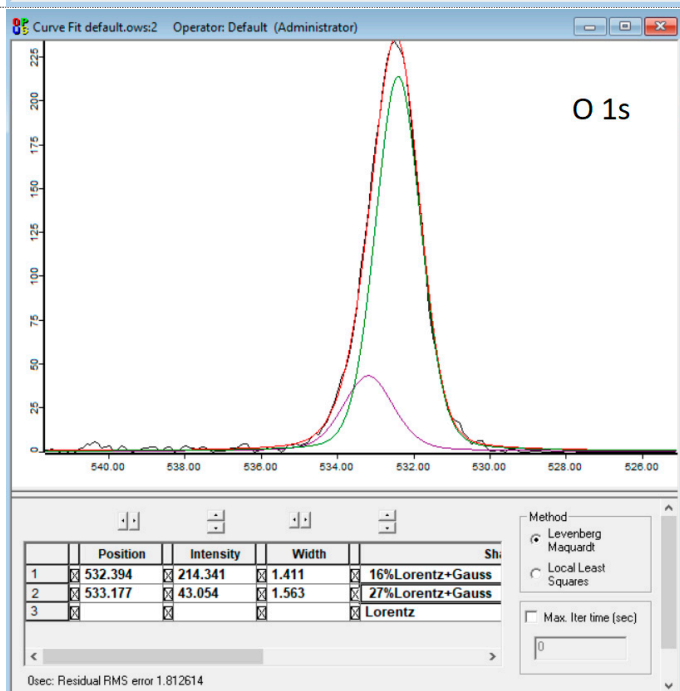
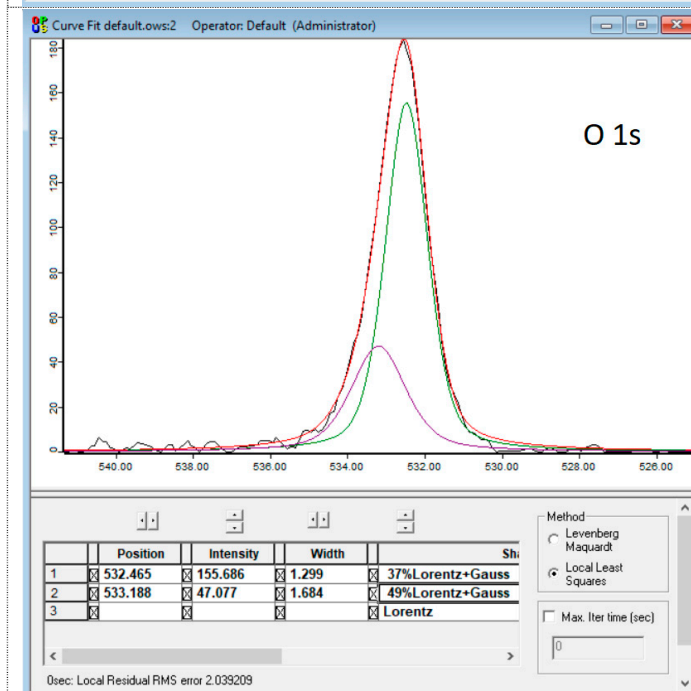
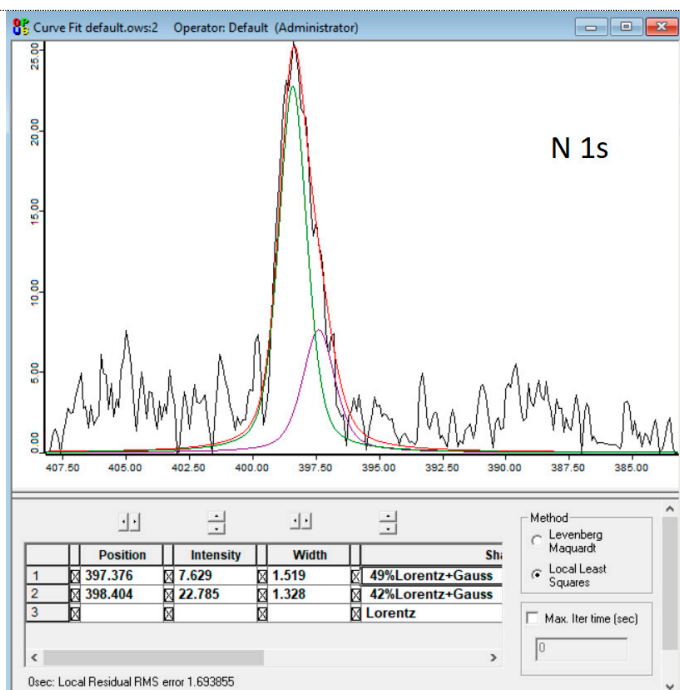
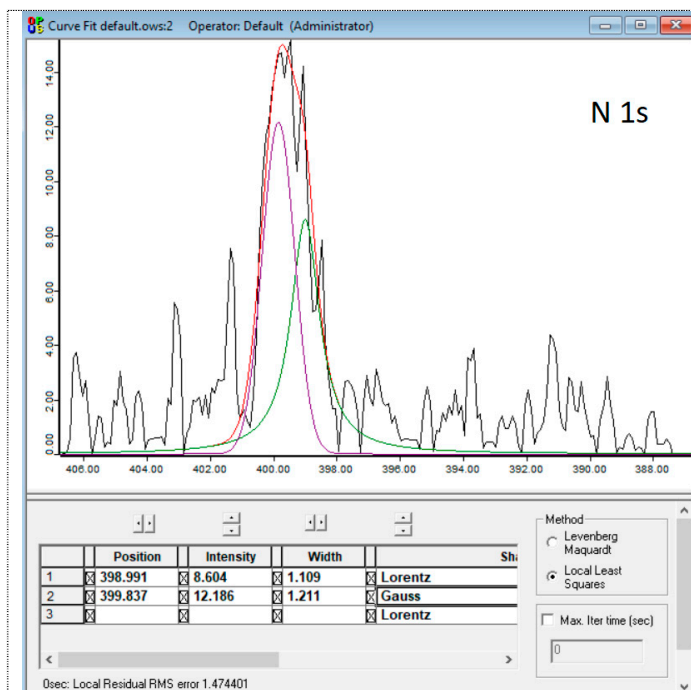
$\alpha = 1$

X = TFSI⁻



X = Triflate⁻





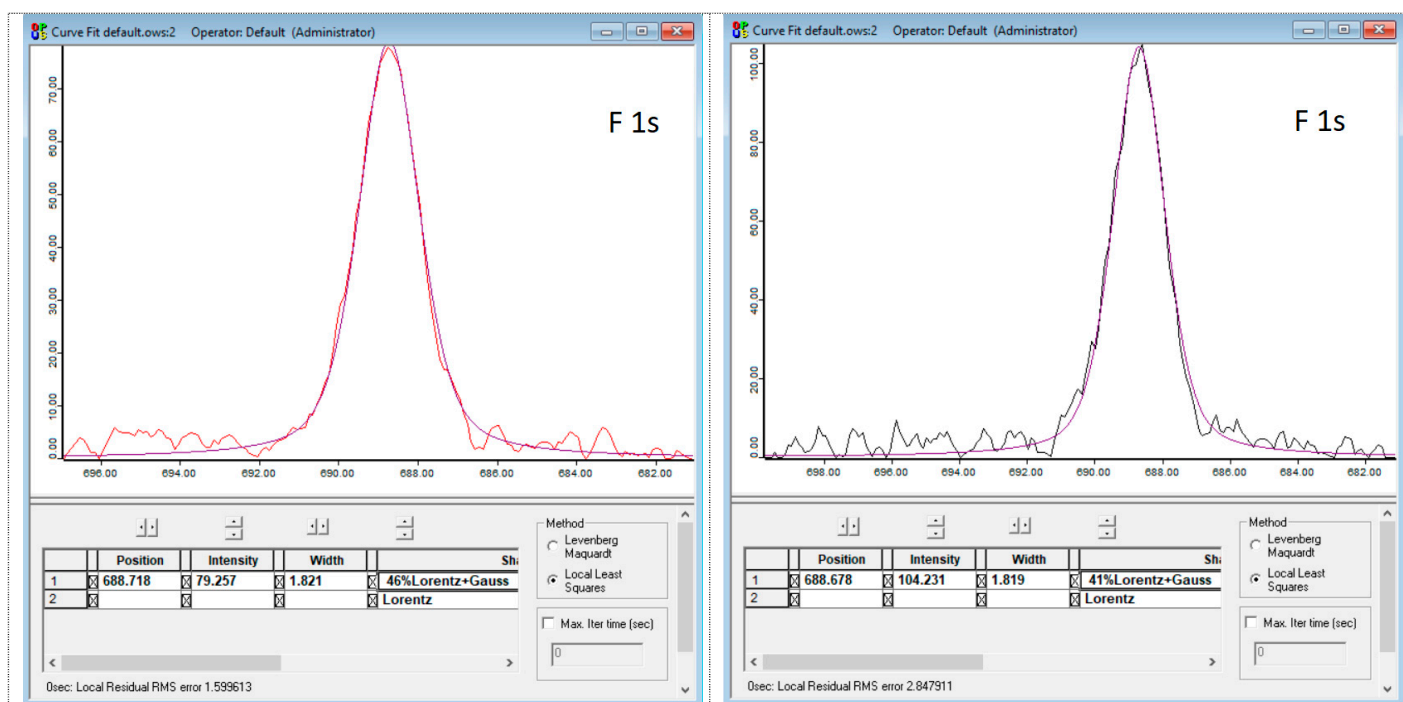


Figure S5. Best fits of XPS spectra of different elements of solid redox mediators ($x = 1$; X = TFSI⁻ and Triflate⁻).

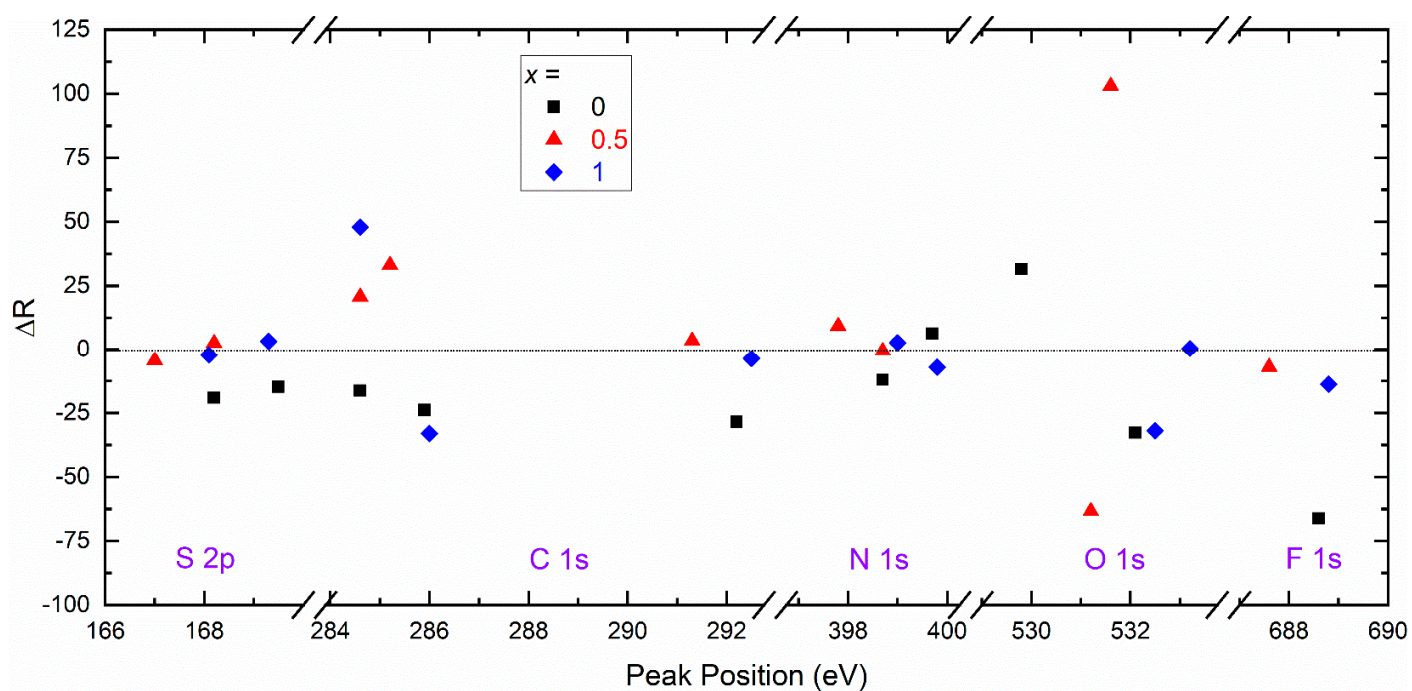


Figure S6. A plot of ΔR ($= [\text{intensity/width}]_{\text{TFSI}} - [\text{intensity/width}]_{\text{Triflate}}$) with peak position for different elements of solid redox mediators, $[(1-x)\text{SN}: x\text{PEO}]\text{-LiX-Co}$ salts, where $x = 0, 0.5$, and 1 . $X = \text{TFSI}^-$ and Triflate^- .

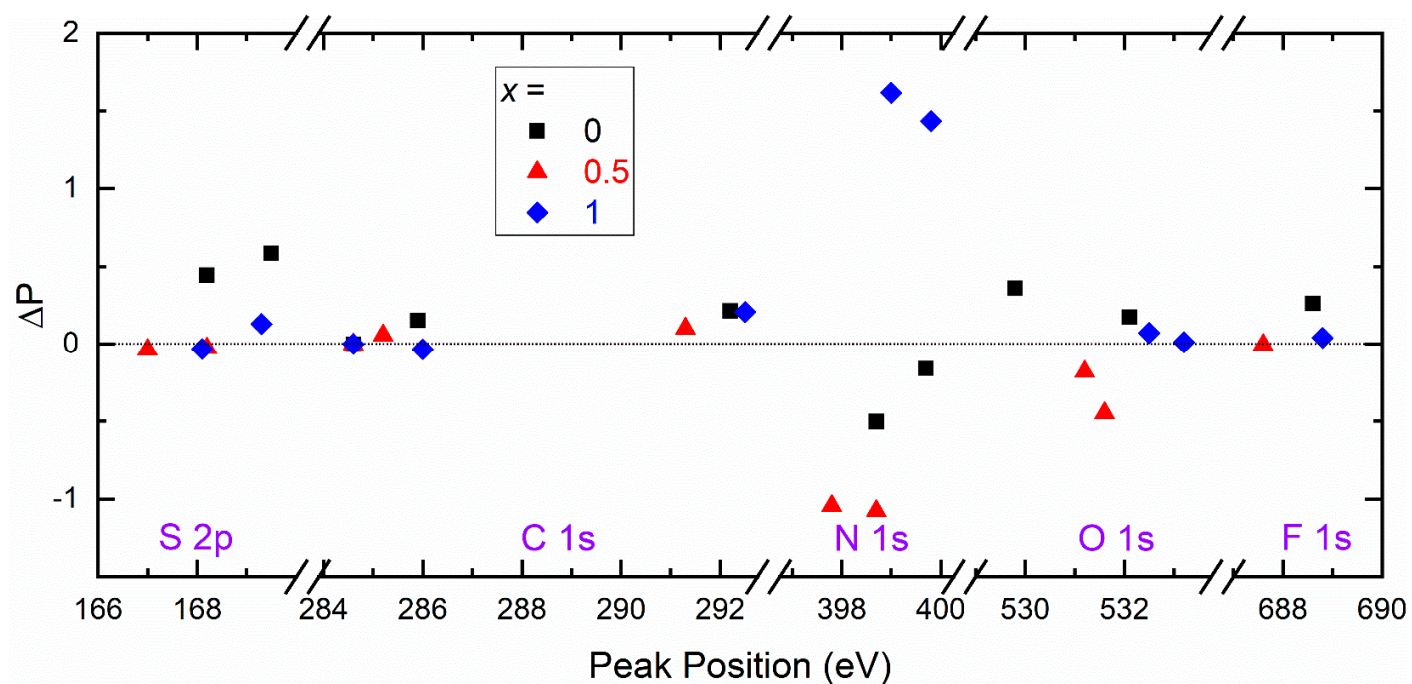


Figure S7. A plot of ΔP ($= [\text{peak position}]_{\text{TFSI}} - [\text{peak position}]_{\text{Triflate}}$) with peak position for different elements of solid redox mediators, $[(1-x)\text{SN}: x\text{PEO}]\text{-LiX-Co}$ salts, where $x = 0, 0.5$, and 1 . $X = \text{TFSI}^-$ and Triflate^- .